Point-Cloud-to-Point-Cloud Technique on Tool Calibration for Dental Implant Surgical Path Tracking

Auranuch Lorsakul[1], Jackrit Suthakorn*[,1] and Chanjira Sinthanayothin[2]
[1]Department of Biomedical Engineering, Center for Biomedical and Robotics Technology, Faculty of Engineering, Mahidol University, THAILAND
[2]Advanced Dental Technology Center, National Science and Technology Development Agency, THAILAND
*Corresponding Author: egjst@mahidol.ac.th

ABSTRACT

Dental implant is one of the most popular methods of tooth root replacement used in prosthetic dentistry. Computerize navigation system on a pre-surgical plan is offered to minimize potential risk of damage to critical anatomic structures of patients. Dental tool tip calibrating is basically an important procedure of intraoperative surgery to determine the relation between the hand-piece tool tip and hand-piece's markers. With the transferring coordinates from preoperative CT data to reality, this parameter is a part of components in typical registration problem. It is a part of navigation system which will be developed for further integration. A high accuracy is required, and this relation is arranged by point-cloud-to-point-cloud rigid transformations and singular value decomposition (SVD) for minimizing rigid registration errors.

In earlier studies, commercial surgical navigation systems from, such as, BrainLAB and Materialize, have flexibility problem on tool tip calibration. Their systems either require a special tool tip calibration device or are unable to change the different tool.

The proposed procedure is to use the pointing device or hand-piece to touch on the pivot and the transformation matrix. This matrix is calculated every time when it moves to the new position while the tool tip stays at the same point. The experiment acquired on the information of tracking device, image acquisition and image processing algorithms. The key success is that point-to-point-cloud requires only 3 post images of tool to be able to converge to the minimum errors 0.77%, and the obtained result is correct in using the tool holder to track the path simulation line displayed in graphic animation.

Keywords: Tool tip calibration, Navigation System, Optical Tracking, Point-Cloud-to-Point-Cloud Rigid Transform

1. INTRODUCTION

Dental Implant is the most frequent method of tooth root replacement used in prosthetic dentistry. Computerize navigation system is offered to minimize potential risk of damage to critical anatomic structures of patients. The methodology based on CIS interventions includes preoperative and intraoperative procedures. The preoperative surgery is to use 3D views as provided to enhance raw images obtained from the patient before operation. This helps to get familiar with the anatomy of the patient. The techniques are to render a target region and a pathway associated with relative organs from CT data. While intraoperative support can be used during the real surgical procedure both a navigation and a decision aid. The tracking systems, which consist of a calibrated stereo scope, and two sets of special designed reference markers attached on the dental hand-piece tool and patient's jaw, are associatively registered together in the system.

Dental tool tip calibrating is basically an important procedure to determine the relation between the hand-piece tool tip and hand-piece's markers which can be formed as vector btip. Regarding to transferring coordinates from preoperative data to reality, this parameter is a part of significant component in typical registration problem.

Earlier studies for tool tip calibration are developed and implemented by some commercial surgical navigation systems, such as, Medtronics, GE, BrainLAB Vector Vision, and Materialize. BrainLAB uses technique of digitizing a tool tip on CT image and based on database. Therefore, the drawback of this system is lack of flexibility in changing different tools.

Moreover, the BrainLAB system utilizes and relies on a big stack of databases which might not be truly reliable. It has been an argument that the databases were collected from Europeans which might be problematic to Asians. Materialize calibrates tool tips by posting the instruments equipped with markers into a specific tool calibrating jig furnished with a reference marker. This method requires the mention specific tool which less flexibility.

The objective of this paper is to implement point-cloud-to-point-cloud technique to indicate tool tip for the instrument calibration process. This method is promising method to require only a few tool posts per tool tip calibration. Because of high accuracy requirement, a transformation matrix is proposed to arrange by point-cloud-to-point-cloud rigid transformations and singular value decomposition (SVD). With these algorithms, they can substantially minimize rigid registration errors [1], [2]. The experiment results are compared to the earlier tool tip calibration algorithm and are simulated by a path tracking from obtained relationship.

1.1 System Description of Tool Tip Calibration

1.1.1 Calibration Concept

The idea is to use the pointing device calibration technique to find the homogenous transformation matrix between the two sets of IR-LED markers, which attached to the end of the tool holder, and the tip of the instrument. This relationship has a lot of influences in the navigation system as illustrated in Fig. 1. This parameter fulfills the navigation path from CT data to the tool tip of the instrument $\mathbf{F}_{Ctip}$. The relationship $\mathbf{F}_{Ctip}$ can be calculated by

$$\mathbf{F}_{Ctip} = \mathbf{F}_{reg}\mathbf{F}^{-1}_{ref}\mathbf{F}_{tool}\mathbf{F}_{tip} \tag{1}$$

where $\mathbf{F}_{reg}$ is the registration transformation between the CT data frame and reference frame, $\mathbf{F}^{-1}_{ref}$ is the inversion of the reference transformation with respect to the camera frame, $\mathbf{F}_{tool}$ is the tool transformation between tool's marker frame and the camera frame, and $\mathbf{F}_{tip}$ is the tool tip transformation between the tool's marker frame and tool tip.

The principal procedure to find the $\mathbf{F}_{tip}$ is that to use the pointing device or hand-piece to touch the point on the pivot and the transformation matrix. The transformation matrix is calculated every time when it moves to new positions while the tool tip stays at the same point on pivot. This matrix is formed by 3x3 rotation matrix, **R**, and translation vector, **p**. Rotation matrix described a frame rotated which relates to the reference frame, and for translation vector, it uses for interpreting of actually translating the point in space.

Tool tip calibration is one of modules in navigation system. Fig. 2 shows the block diagram of the overall system. This system is basically based on optical tracking which is used to obtain images that are retrieved by stereo camera. Tool tip parameter is an important key to fulfill the navigation system path. This parameter informed the end effecter of dental tool instrument relative to the fiducial marker. In the real time circumstance, the tool calibration procedure is performed before using the guided system. Furthermore, there is another tool, digitizer which is used for digitizing the significant position of the patient's anatomy relative to CT images, has to be calibrated similarly. After that the patient's CT data will be loaded into the program, then the attractive graphic animation of the surgical tool with accurate end effecter displayed relatively to the patient's CT data. Therefore, the more accurate end effecter determination, the more precise navigation will be obtained. This calibration method in this paper is a new concept in tool tip's end effecter determination by using a mathematic algorithm, point-cloud-to-point-cloud and SVD.

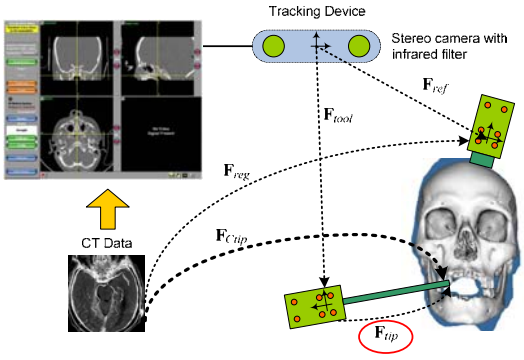

$\mathbf{F}_{Ctip} = \mathbf{F}_{reg}\mathbf{F}^{-1}_{ref}\mathbf{F}_{tool}\mathbf{F}_{tip}$

Fig. 1. Navigation System Diagram

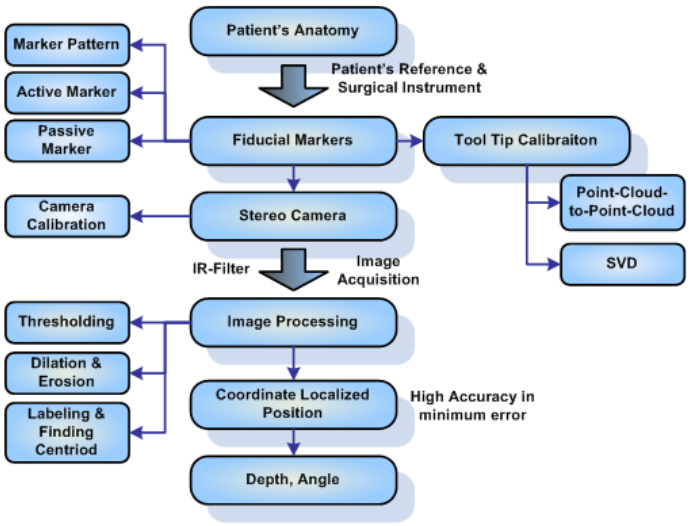

Fig. 2 Methodology diagram of navigation system

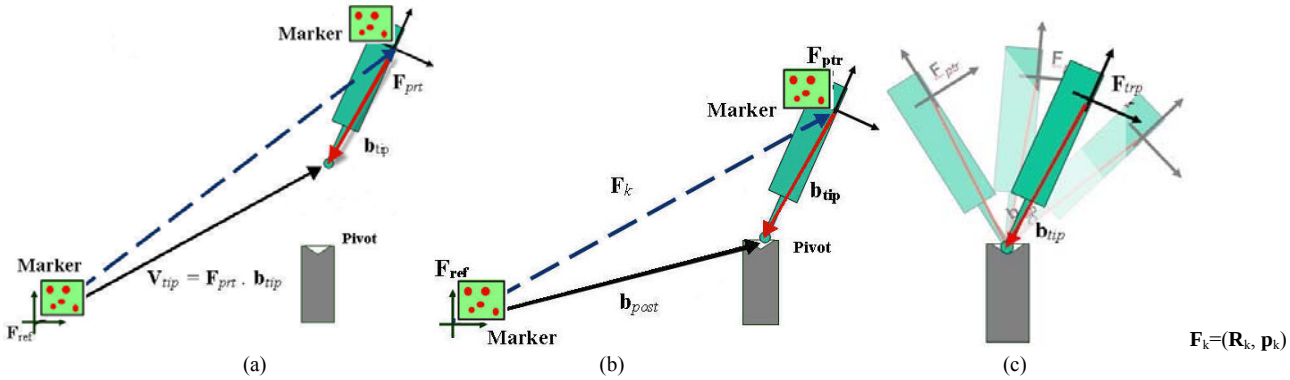

Fig. 3. Pointing Device Calibration Technique (a) Vectors relationship between two frames of markers, (b) Position of the instrument while calibrating , (c) Various post positions for finding the transformation matrix

Fig. 3 shows the method used to find the vector $\mathbf{b}_{tip}$, which represents the relationship between tool's marker and tool tip.

For each measurement *k*, we have

$$\vec{\mathbf{b}}_{post} = \mathbf{R}_k \vec{\mathbf{b}}_{tip} + \vec{\mathbf{p}}_k . \tag{2}$$

With new arrangement,

$$\mathbf{R}_k \vec{\mathbf{b}}_{tip} - \vec{\mathbf{b}}_{post} = -\vec{\mathbf{p}}_k . \tag{3}$$

Set up a least square problem

$$\begin{bmatrix} \vdots & \vdots \\ \mathbf{R}_k & -\mathbf{I} \\ \vdots & \vdots \end{bmatrix} \begin{bmatrix} \vec{\mathbf{b}}_{tip} \\ \vec{\mathbf{b}}_{post} \end{bmatrix} \cong \begin{bmatrix} \mathrm{M} \\ -\vec{\mathbf{p}}_k \\ \mathrm{M} \end{bmatrix} \tag{4}$$

This can be represented as $\tilde{\mathbf{A}}\tilde{\mathbf{b}} = \tilde{\mathbf{p}}$ and the required vector can be written as $\tilde{\mathbf{b}} = (\tilde{\mathbf{A}}^T\tilde{\mathbf{A}})^{-1}\tilde{\mathbf{A}}^T\tilde{\mathbf{p}}$, and $(\tilde{\mathbf{A}}^T\tilde{\mathbf{A}})^{-1}\tilde{\mathbf{A}}^T$ is called as pseudo inversion

where $\tilde{\mathbf{A}} = \begin{bmatrix} \vdots & \vdots \\ \mathbf{R}_k & -\mathbf{I} \\ \vdots & \vdots \end{bmatrix}$, $\tilde{\mathbf{b}} = \begin{bmatrix} \vec{\mathbf{b}}_{tip} \\ \vec{\mathbf{b}}_{post} \end{bmatrix}$, and $\tilde{\mathbf{p}} = \begin{bmatrix} \mathrm{M} \\ -\vec{\mathbf{p}}_k \\ \mathrm{M} \end{bmatrix}$.

1.1.2 System Overview

Fig. 4 illustrates the system configuration. The calibrated stereo cameras with infrared filter are used to retrieve images. The Image Acquisition has been implemented to capture monochrome image through MATLAB®. Each post measurement, k, has been stored by image processing module. Every single image has been processed by Image Processing module. The obtained 3D coordinates of marker positions are accomplished by thresholding and morphological image processing techniques in order to complete the structuring elements of object region. After that, all centroids of marker region in the left and the right stereo images as well as intrinsic and extrinsic stereo parameters are input into stereo triangulation function. Then, the 3D positions which are equivalent to the world coordinate system are obtained. With these two sets of point cloud of the two markers, the transformation matrix is calculated by SVD principle and achieves desired parameters.

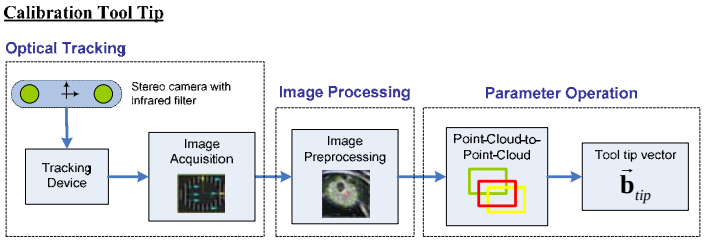

Fig. 4. System Overview

1.2 Optical Tracking and Image Processing Stage

1.2.1 Optical Tracking

1) Stereo Camera Calibration: The stereo camera calibration has been performed by Stereo Camera Calibration Toolbox for MATLAB® which is based on planar checkerboard. Fig. 5 illustrates Left and Right images used for camera calibration. The initial values of the intrinsic and extrinsic camera parameters are determined in order to characterize the relative location of the right camera with respect to the left camera. This process is known as stereo triangulation [8], [9]. In this paper, the 3D coordinates of the position obtained from left camera are set to be a reference frame of the system.

2) Tracking Device: The active IR-LED optical tracking devices are utilized as markers or object trackers. The main purpose of a tracking system is to determine the 3D coordinate of an object [11]. The benefit of infrared optical tracking system is to extract the differences between markers and background. The objects except the surgical markers in the operation room become invisible. The two sets of active markers are setup as reference frame, $\mathbf{F}_{ref}$, and another one is jigged on the top of the tool holder which is called the pointing frame, Fptr. With these two sets of markers, they represent the two set of point clouds $\{a_i\}$ and $\{b_i\}$ as illustrated in Fig. 6

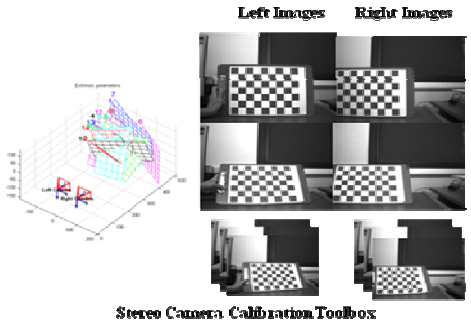

Fig. 5 illustrates Left and Right images used for camera calibration and based on planar checkerboard principle

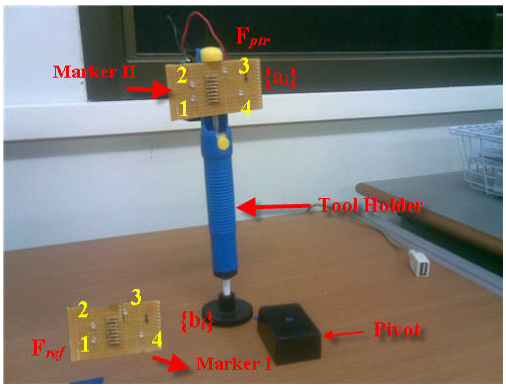

Fig. 6. Example of marker and tool holder

3) Image Acquisition: This is the first stage of the vision system. Basically, Bumblebee camera connects to a PC transmission via an IEEE-1394 interface (FireWire). The image is satisfactorily obtained by software, which is implemented together with Digiclops® and Triclops, Bumblebee Library, for capturing monochrome images through MATLAB® [12]. While calibrating, the left and right images are necessary to be snapshot simultaneously in each pool of measurement. The examples of image which pass IR-Filter is illustrated in Fig. 7(a) and 5(b).

1.2.2 Image Processing

When the images have been acquired satisfactorily, the intended tasks are achievable with the aid of some form of image enhancement. The techniques that employed in this paper are Thresholding, Dilation and Erosion, and Labeling and Finding Centroid. Each image is processed to obtain the 3D coordinates of marker positions. Thresholding and morphological image processing techniques have been performed to complete the structuring elements of object region. All centroids of marker region in left and right stereo images, and intrinsic and extrinsic stereo parameters are input into stereo triangulation function to find the 3D positions which are equivalent to the world coordinate system.

1) Thresholding: The acquired images are converted into binary images by thresholding technique. Thresholding is a method to distinguish the required objects in an image from background by creating a binary partitioning of the image intensities. The procedure is accomplished by comparing to the desired intensity value called threshold to intensities of all pixels in the image. The pixels that have intensity value greater than the threshold are assigned to one class. Otherwise, they are assigned to another class [11].

2) Dilation and Erosion: The use of combination of dilation and erosion, together with opening and closing, is employed to enhance the structure of the interesting regions. Dilation is to gradually enlarge the boundaries of regions of foreground pixels. Opening tends to remove some of the foreground pixels from the edges of regions of foreground pixels, while closing inclines to enlarge the boundaries of foreground regions in an image, but it is less destructive of the original boundary shape [13].

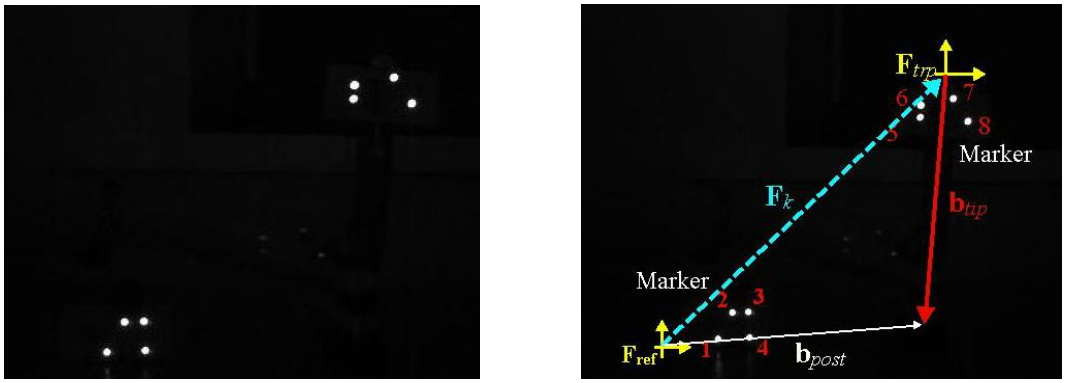

(a) (b)

Fig. 7. (a) Example of capture image from camera, (b) Graphic indicates the components of pointing calibrated technique

3) Labeling and Finding Centroid: With these improved regions in images, the centroids of the objects presented in both left and right images are calculated. Before finding centroids, the connected components labeling is performed by scanning an image and groups its pixels into components based on pixel connectivity. All pixels in a connected component have the same intensity values and connect to each other through its neighbors. After the labeling is performed to locate the area of markers, centroids of markers are determined to represent the position of the marker accordingly.

1.3 Parameter Operation Stage

1.3.1 Point-Cloud-to-Point-Cloud Rigid Transformation

Typically, a set of points $\{a_i\}$ in one coordinate system and another set of points $\{b_i\}$ in a second coordinate system are given. The goal is to find [**R**,**p**] that minimize

$$\eta = \sum_i e_i \bullet e_i \quad \text{, where } e_i = (\mathbf{R} \bullet a_i + \mathbf{p}) - b_i \tag{5}$$

To find the least-squares solution of **R** and **T**, the centroids of each point cloud and SVD of a rotation matrix are perform as following algorithms.

1.3.2 Algorithm to find rigid transformations

Step 1: Compute centroid of each point cloud

$$\bar{a} = \frac{1}{N}\sum_{i=1}^{N} \vec{a}_i \qquad \bar{b} = \frac{1}{N}\sum_{i=1}^{N} \vec{b}_i$$

$$\tilde{a}_i = \vec{a}_i - \bar{a} \qquad \tilde{b}_i = \vec{b}_i - \bar{b}$$

Step 2: Find R that minimizes

$$\sum_i (\mathbf{R} \cdot \tilde{a}_i - \tilde{b}_i)^2$$

Step 3: Find $\vec{\mathbf{p}}$

$$\vec{p} = \bar{b} - \mathbf{R} \cdot \bar{a}$$

Step 4: Desired transformation is

$$\mathbf{F} = Frame(\mathbf{R}, \vec{\mathbf{p}})$$

*1.3.3 Algorithm to find minimized rotation **R***

Basically, there are many ways to find rotation matrix **R** that minimize $\sum 2$ such as quaternion, iterative and noniterative techniques. In this study, we selected noniterative algorithm involved with the singular value decomposition (SVD) of a 3x3 matrix because this method can be performed fastest with high accuracy compared to the quaternion and iterative methods. The algorithm can be shown:

Step 1: Compute

$$\mathbf{H} = \sum_i \begin{bmatrix} \bar{a}_{i,x}\bar{b}_{i,x} & \bar{a}_{i,x}\bar{b}_{i,y} & \bar{a}_{i,x}\bar{b}_{i,z} \\ \bar{a}_{i,y}\bar{b}_{i,x} & \bar{a}_{i,y}\bar{b}_{i,y} & \bar{a}_{i,y}\bar{b}_{i,z} \\ \bar{a}_{i,z}\bar{b}_{i,x} & \bar{a}_{i,z}\bar{b}_{i,y} & \bar{a}_{i,z}\bar{b}_{i,z} \end{bmatrix}$$

Step 2: Compute the SVD of $\mathbf{H}=\mathbf{U}\mathbf{S}\mathbf{V}^{\mathbf{t}}$

Step 3: $\mathbf{X}=\mathbf{U}\mathbf{V}^{\mathbf{t}}$

Step 4: Verify *Det*(**X**)

If *Det*(**X**) = +1, then **X** is rotation (**R=X**), and If *Det*(**X**) = -1, **X** is a reflection.

In case that X is a reflection, then $\mathbf{R}=\mathbf{V}'\mathbf{U}^{t}$, where $\mathbf{V}' = [v_1, v_2, -v_3]$. This can be proved in method due to K. Arun, *et. al* [1]. Table 1 is the summary of the algorithms to find the rigid transformation and minimized rotation.

Table 1 Algorithms to find rigid transformation and minimized rotation

Algorithms to find rigid transformations	Algorithms to find minimized rotation R
Step 1: Compute centroid of each point cloud $\bar{a}=\frac{1}{N}\sum_{i=1}^{N}\vec{a}_i$ $\bar{b}=\frac{1}{N}\sum_{i=1}^{N}\vec{b}_i$ $\tilde{a}_i=\vec{a}_i-\bar{a}$ $\tilde{b}_i=\vec{b}_i-\bar{b}$ *Step 2*: Find R that minimizes $\sum_i(\mathbf{R}\cdot\tilde{a}_i-\tilde{b}_i)^2$ *Step 3*: Find $\vec{p}$ $\vec{p}=\bar{b}-\mathbf{R}\cdot\bar{a}$ *Step 4*: Desired transformation is F=*Frame*(R, $\vec{p}$)	*Step 1*: Compute $\mathbf{H}=\sum_i\begin{bmatrix}\bar{a}_{i,x}\bar{b}_{i,x} & \bar{a}_{i,x}\bar{b}_{i,y} & \bar{a}_{i,x}\bar{b}_{i,z}\\ \bar{a}_{i,y}\bar{b}_{i,x} & \bar{a}_{i,y}\bar{b}_{i,y} & \bar{a}_{i,y}\bar{b}_{i,z}\\ \bar{a}_{i,z}\bar{b}_{i,x} & \bar{a}_{i,z}\bar{b}_{i,y} & \bar{a}_{i,z}\bar{b}_{i,z}\end{bmatrix}$ *Step 2*: Compute the SVD of H=USV^t *Step 3*: X=UV^t *Step 4*: Verify *Det*(X) If *Det*(X) = +1, then X is rotation (R=X). If *Det*(X) = -1, X is a reflection. In case that X is a reflection, then R=V'U^t, where V' = $[v_1 \quad v_2 \quad -v_3]$.

1.4 Experiment Result and Analysis

1.4.1 Tools and Equipments

1. Bumblebee2® stereo vision camera system (BB2-BW-60), monochrome, 640x480 at 48 FPS, 6.0 mm focal length lens, two 1/3" progressive scan CCD sensors, and both the left and right images to a PC transmission via an IEEE-1394 interface.
2. Infrared filter covers the stereo cameras
3. Two markers with 4-IR-LEDs for each
4. Pivot
5. Tool Holder
6. MATLAB® program for calculation
7. Camera Calibration Toolbox for MATLAB®

1.4.2 Simulation and Results

1) Testing calibration with standard calibration: This experiment has been implemented and compared to the same method as Materialize. After captured the various position of the instruments which attached with the tracking devices, then the left and right images have been captured and processed by image processing section. The positions of objects with respect to three-dimensional coordinates are performed as set of point clouds $\{a_i\}$ and $\{b_i\}$. $[\mathbf{R},\mathbf{p}]$ is calculated by the least square problem setting up in order to compute $\mathbf{b}_{tip}$ in $\tilde{\mathbf{b}} = (\tilde{\mathbf{A}}^T\tilde{\mathbf{A}})^{-1}\tilde{\mathbf{A}}^T\tilde{\mathbf{p}}$. The Euclidean distance is calculated as a distance between two points from this study and Materialize methods as the following relationship:

$$d(\mathbf{x},\mathbf{y}) = \|\mathbf{x}-\mathbf{y}\| = \sqrt{(x_1-y_1)^2+(x_2-y_2)^2+(x_3-y_3)^2}\,, \tag{10}$$

where **x** and **y** are any two points [8].

The Spatial Error and Euclidean distances compared with Materialize in 17 post measurements are shown in Table 2. Fig 8. displays graph plot of Euclidean distances between the results from this study and the results from Materialize method.

For Materialize method, it can be simply determined by directly counting pixels or calculating vector positions. The tip of the tool will be fixed to a host position and will be measured the end effecter directly without movement to new positions. According to the spatial errors and Euclidean distance comparison, this study accomplishes in terms of accuracy and precision. This method can be performed only three post measurements to achieve the minimize errors which is more efficient than BrainLAB method which depended on a certain amount of database.

TABLE 2

Comparison of results in terms of spatial errors (mm) and Euclidean distance between this study and Materialize method.

No. of Post	Spatial Errors (mm)	Euclidean Distance Between Two Methods
1	(-0.4024, -1.056, 1.4923)	1.8719
2	(-0.6785, 0.5637, 0.3981)	0.9677
3	(0.0082, 0.0031, 0.0047)	0.0100
4	(0.0170, -0.0015, 0.0074)	0.0185
5	(0.0171, -0.0015, 0.0074)	0.0187
6	(0.0172, -0.0015, 0.0075)	0.0188
7	(0.0174, -0.0016, 0.0076)	0.0191
8	(0.0184, -0.002, 0.0079)	0.0201
9	(0.0176, -0.0017, 0.0076)	0.0193
10	(0.0173, -0.0016, 0.0075)	0.0189
11	(0.0174, -0.0016, 0.0075)	0.0190
12	(0.0173, -0.0017, 0.0075)	0.0190
13	(0.0173, -0.0017, 0.0075)	0.0189
14	(0.0175, -0.0017, 0.0075)	0.0191
15	(0.0172, -0.0016, 0.0075)	0.0188
16	(0.0173, -0.0017, 0.0075)	0.0189
17	(0.0173, -0.0016, 0.0075)	0.0189

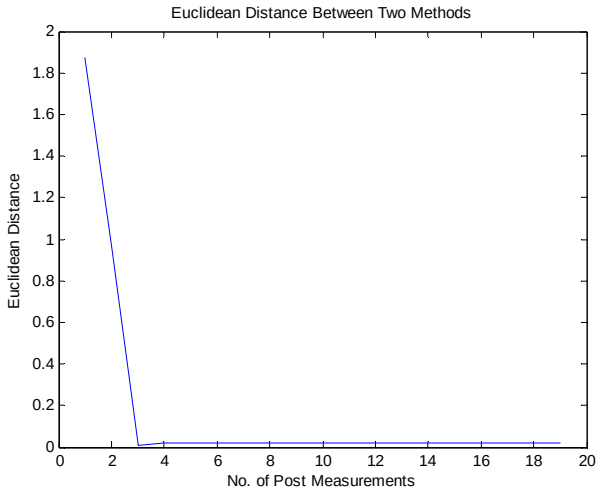

Fig. 8. Euclidean distance between this study and Materialize method.

2) Testing calibration with tracking system: The tracking simulation has been performed by using the $\mathbf{b}_{tip}$ that obtained from tool tip calibration by point-cloud-to-point-cloud method. The animation of relationship between marker position and tool tip is established by simulation on MATLAB®. Fig 9 illustrated the system concept in tracking simulation.

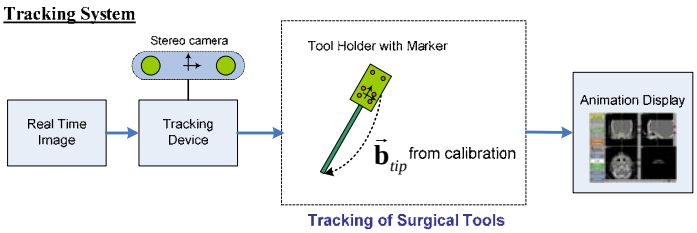

Fig. 9. Tracking system simulation concept.

The simulation environment setup is established. Vector $\mathbf{b}_{mark}$ is the information that obtains from image processing stage. Vector $\mathbf{b}_{res}$ can be calculated by the relationship as equation (11). Fig. 10 (a) displays the model relationship among vectors with respect to the camera frame.

$$\mathbf{b}_{res} = \mathbf{b}_{mark} + \mathbf{R}_{mark} \cdot \mathbf{b}_{tip}, \tag{11}$$

where $\mathbf{R}_{mark}$ is rotation matrix which is an orientation between a point on the marker in space that attaches a marker coordinate system relative to the reference system on camera.

This rotation matrix, $\mathbf{R}_{mark}$ can be calculated by unit vectors on camera coordinate system and marker coordinate system as shown in equation (8) and illustrated in Fig. 10 (b).

$$\mathbf{R}_{mark} = \begin{bmatrix} \hat{X}_B \cdot \hat{X}_A & \hat{Y}_B \cdot \hat{X}_A & \hat{Z}_B \cdot \hat{X}_A \\ \hat{X}_B \cdot \hat{Y}_A & \hat{Y}_B \cdot \hat{Y}_A & \hat{Z}_B \cdot \hat{Y}_A \\ \hat{X}_B \cdot \hat{Z}_A & \hat{Y}_B \cdot \hat{Z}_A & \hat{Z}_B \cdot \hat{Z}_A \end{bmatrix}, \tag{12}$$

where $\hat{X}_A, \hat{Y}_A$, and $\hat{Z}_A$ are unit vectors that are denoted to give the principal directions of reference coordinate system on camera.

$\hat{X}_B, \hat{Y}_B$, and $\hat{Z}_B$ are unit vectors that are denoted to give the principal directions of marker coordinate system on the tool.

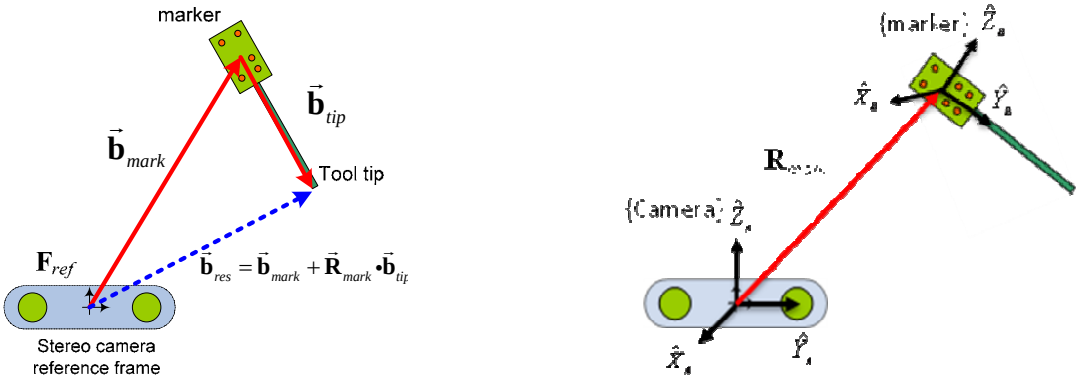

(a) (b)

Fig. 10 (a) Model of relationship among vectors with respect to the camera frame, and (b) Locating reference coordinate system on camera and marker coordinate system on the tool

In a Graphic User Interface, it displays after running program. The displayed GUI consists of components below and illustrates in Fig. 11 which shows the display GUI of Optical Tracking System. The GUI consists of component for displaying significant graphic and parameters of optical tracking system as follows:

- 3-D Coordinate display
- Left camera image display

- Right camera image display
- Camera operation
- Marker notification
- Transformation detail

After running the program, the GUI display, and then click at “Open Camera” button to retrieve images. The images are displayed in left and right camera areas. The simulation program shows the location of fiducial marker in the camera space. 3-D coordinate plot is displayed on the animation area subsequently. This animation is the simple prototype to display position and orientation of the surgical tool after performing tool tip calibration. The obtained parameter, $\mathbf{b}_{tip}$, is composed together with the position of the marker to be a rigid tool and displays accordingly in GUI window.

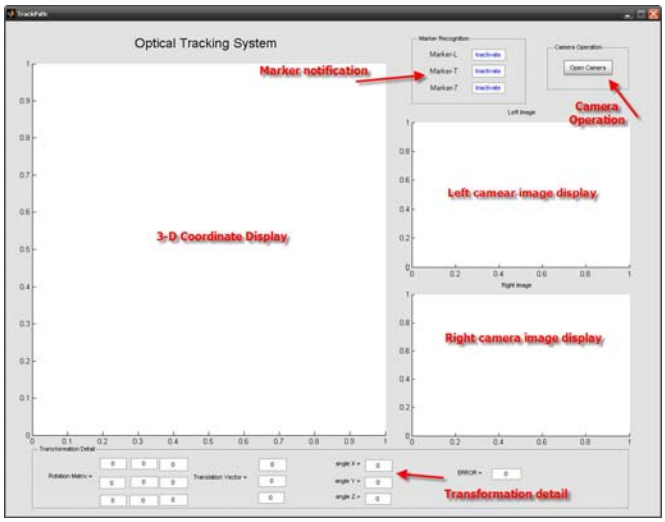

Fig. 11 shows Layout of display GUI after running program

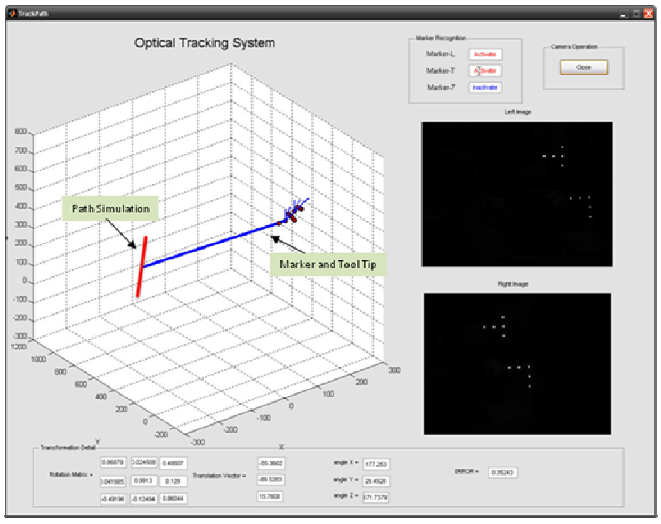

Fig. 12. Tracking Path Animation

Fig. 13. System environment setup

The experiment has been arranged by using the tool tracks the path simulation in the workspace in MATLAB® as shown in Fig. 12. The simulation environment setup is shown in Fig. 13. The obtained result is correct in using the tool holder to track the path simulation line displayed in graphic animation. In operation aspect, this path simulation can be assumed as the guided navigated path in surgical operation. The tool holder is equivalent to hand-piece for dentist that utilized for drilling patient's jaw in the dental implant operation.

1.5 Conclusion

This paper gives a systemic introduction about our ongoing project, the dental navigation system. In this work, we construct and fulfill some simple experiments on tool tip calibration with Point-Cloud-to-Point-Cloud technique and the Least-Square Solution which compared to the earlier tool tip calibration method and be able to obtain satisfied error. For tracking simulation, it found that this relation is able to accomplish to track the path simulation which assumed as the guidance in navigation system. The experiment acquired the information of tracking device, image acquisition and image processing algorithm. The key success is that point-to-point-cloud requires only 3 post images of tool to be able to converge to the minimum errors while BrainLAB needs a lot more.

Future tasks consist of the integrated system with preoperative surgery and intraoperative tracking systems. A series of experiments of overall system will be carried out in order to validate the performance of the system and algorithm.

REFERENCES

[1] K. S. Arun, T. S. Huang, and S. D. Blostein, "Least-Squares Fitting of Two 3-D Point Sets", IEEE Transactions on Pattern Analysis And Machine Intelligence, Sep. 1987, pp.698-670.

[2] R. Taylor "Computer-Integrated Surgery" (http://www.cisst.org/~cista/), Engineering Research Center for Computer Integrated Surgical Systems and Technology, Johns Hopkins University, USA.

[3] N. Casap, A. Schnider, and J. Lustmann "Navigation Surgery for Dental Implants: Assessment of Accuracy of the Image Guided Implantology System", American Association of Oral and Maxillofacial Surgeons. 2004:116-9.

[4] B. Jay West and R. Calvin, J. Maurer, "Designing Optically Tracked Instruments for Image-Guided Surgery", IEEE Transaction on Medical Imaging. 2004 January 7;23(5, May 2004):533-45.

[5] N. Casap, N. Persky, A. Schneider, and J. Lustmann. "Navigation Surgery for Dental Implants: Assessment of Accuracy of the Image Guided Implantology System". American Association of Oral and Maxillofacial Surgeons. 2004;62:116-9.

[6] G. Fichtinger, Essential Math for CIS Part 2: Transformations and Frames of Reference]. Available from: http://www.cisst.org/~cista/, 2001.

[7] J. Craig, Introduction to Robotics Mechanics and Control: Pearson Prentice Hall, 2005.

[8] D. Stoyanov, "Camera Calibration Toolbox for Matlab", Royal Society/Wolfson Foundation Medical Image Computing Laboratory, Imperial College London, UK.

[9] P. Eisert, Model-based Camera Calibration Using Analysis by Synthesis Techniques. 2002 November 20-22, 2002.

[10] R. C. Gonzalez, Richard E. Woods, Steven L. Eddins, Digital Image Processing using MATLAB, Pearson Prentice Hall 2004.
[11] T. Kusalanukhun, "Optical Three-Dimensional Coordination for Medical Applications", Master Thesis, Department of Biomedical Engineering, Faculty of Engineering, Mahidol University, Thailand, 2006.
[12] Point Gray Research Inc., "Stereo Vision Product – Digiclops SDK", Available: http://www.ptgrey.com/products/digiclopsSDK/index.asp
[13] B. Fisher, S. Perkins, A. Walker and E. Wolfart, "Hypermedia Image Processing Reference", Department of Artificial Intelligence, University of Edinburgh, UK, Avalable: http://www.cee.hw.ac.uk/hipr/html/hipr_top.html
[14] G. S. Chirikjian, and A. B. Kyatkin "Engineering Applications of Noncommutative Harmonic Analysis: with Emphasis on Rotation and Motion Groups", CRC Press LCC, 2000 N.W. Corporate Blvd., Boca Ration, Florida 3343, p.112, 2001.
[15] B. Fisher SP, A. Walker and E. Wolfart. Connected Components Labeling. 2003 Available from: http://homepages.inf.ed.ac.uk/rbf/HIPR2/label.htm.
[16] L. Iocchi Stereo Vision: Triangulation. Available from: http://www.dis.uniroma1.it/~iocchi/stereo/triang.html.